PNAS
www.pnas.org

Supplementary Information for

Phosphorylation-dependent sub-functionalization of the calcium-dependent protein kinase CPK28

Melissa Bredow, Kyle W. Bender, Alexandra Johnson Dingee, Danalyn R. Holmes, Alysha Thomson, Danielle Ciren, Cailun A. S. Tanney, Katherine E. Dunning, Marco Trujillo, Steven C. Huber, and Jacqueline Monaghan

Dr. Jacqueline Monaghan
jacqueline.monaghan@queensu.ca

This PDF file includes:

Figures S1 to S10
Table S1
SI References

Other supplementary materials for this manuscript include the following:

Datasets S1 to S2

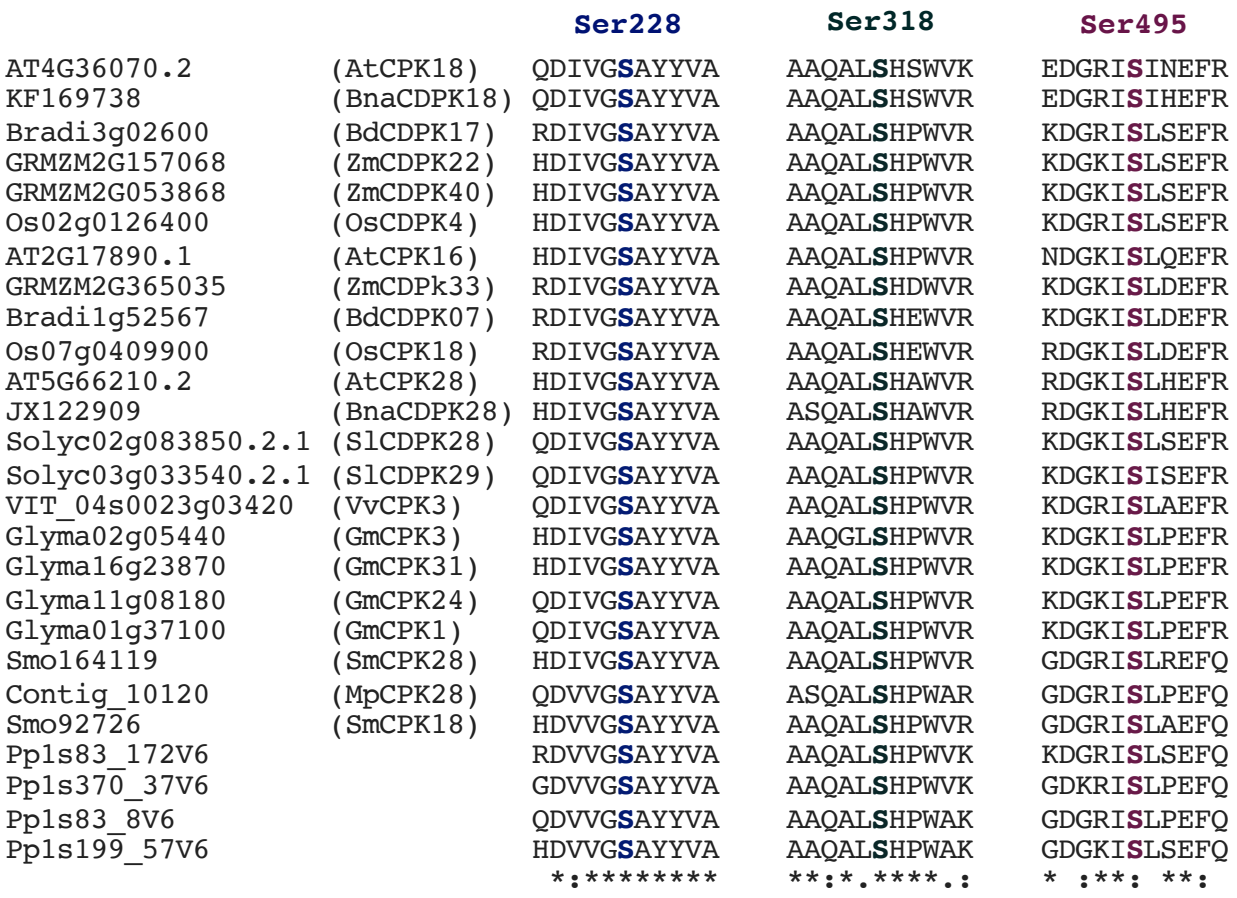

Figure S1. Ser228, Ser318 and Ser495 are conserved across group IV CDPKs. Amino acid sequences of representative group IV CDPKs from eudicots (*Arabidopsis thaliana, Glycine max*, *Solanum lycopersicum*, *Vitis vinifera,* and *Brassica napus)*, monocots *(Brachypodium distachyon*, *Zea mays*, and *Oryza sativa*), bryophytes (*Phsycomiteralla patens)*, liverworts (*Marchantia polymorpha*), and pteridophytes (*Selaginella moellendorffii)* were aligned using Clustal Omega Multiple Sequence Alignment Tool and the residues corresponding to positions 228, 318, and 495 of *Arabidopsis thaliana* CPK28 were compared. "*"=perfect alignment; ":"=strong similarity; "."=weak similarity.

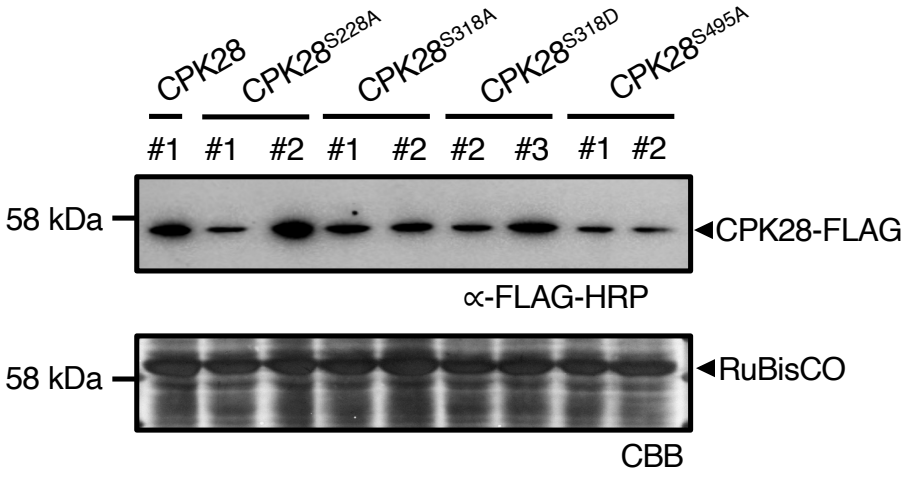

Figure S2. Expression of native promoter-driven CPK28-FLAG phospho-ablative alleles in stable *A. thaliana* lines. Soluble proteins were extracted from 14-day old seedlings grown in MS liquid media and Bradford normalized (4 µg/µL of total protein). Proteins were separated by gel electrophoresis and blotted to PVDF membranes before probing with an anti-FLAG-HRP antibody (1:5,000). PVDF membranes were stained with CBB to ensure equal loading. Experiments were conducted three times with similar results.

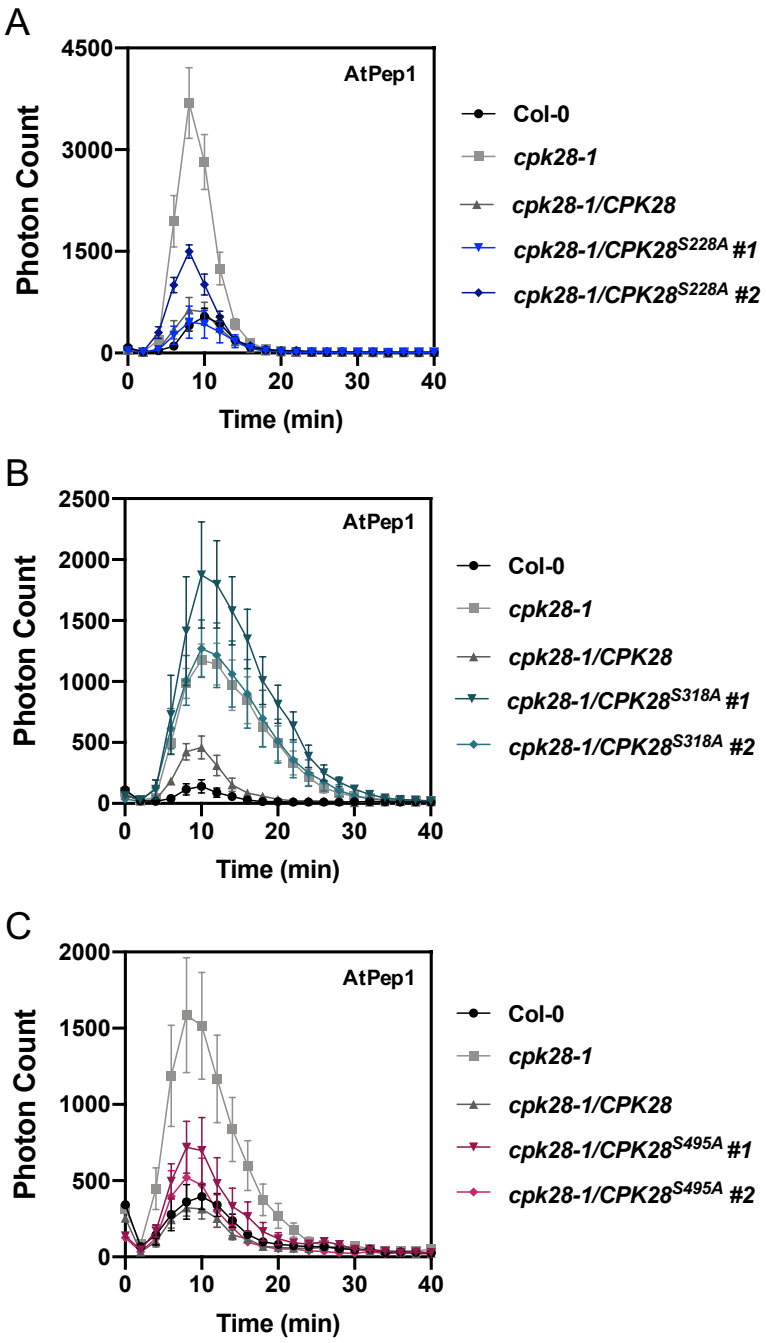

Figure S3. CPK28-Ser318, but not CPK28-Ser228 or CPK28-Ser495, is required for AtPep1-elicited oxidative species production. Oxidative species production in Col-0, *cpk28-1*, *cpk28-1/pCPK28:CPK28-FLAG*, *(A) cpk28-1/pCPK28:CPK28^{S228A}-FLAG, (B) cpk28-1/pCPK28:CPK28^{S318A}-FLAG*, and *(C) cpk28-1/pCPK28:CPK28^{S495A}-FLAG* lines in response to 500 nM AtPep1. Dynamic curves correspond to cumulative photon counts (relative light units) in Figure 1B. Experiments were conducted exactly as described in Bredow et al., 2019 (1) with an integration time of 1000 ms over 40 min with readings every 2 min. Data are presented as means +/- standard error (n=6). Three biological replicates were conducted with similar results.

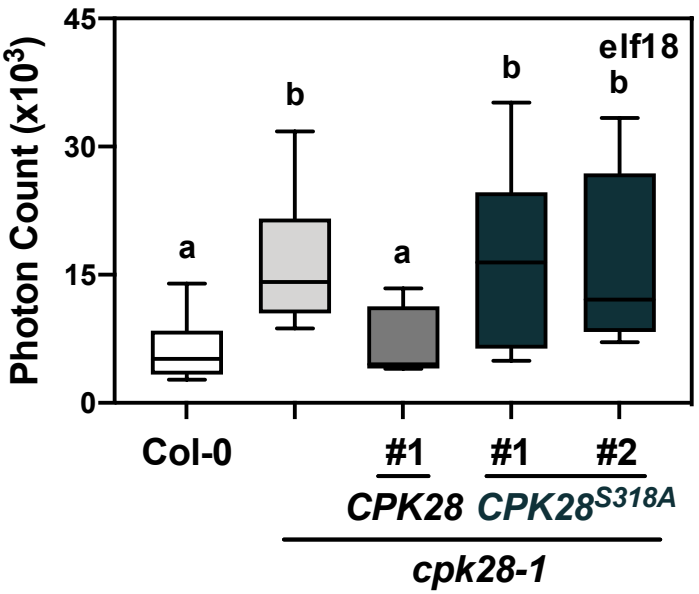

Figure S4. CPK28^{S318A} does not complement *cpk28-1* in response to elf18 treatment. Oxidative bursts of Col-0, *cpk28-1*, *cpk28-1/pCPK28:CPK28-FLAG*, and *cpk28-1/pCPK28:CPK28^{S318A}-FLAG* lines following treatment with 100 nM elf18 (n=6). Values are presented as boxplots indicating first and third quartiles, split by a median line, and whiskers representing maximum and minimum values. Values represent total photon counts over 40 min as described in Bredow et al., 2019 (1) with an integration time of 1000 ms and readings every 2 min. Statistically different groups ($p<0.005$) are indicated with lowercase letters, as determined by one-way ANOVA followed by Tukey's posthoc test. Experiments were conducted three times with similar results.

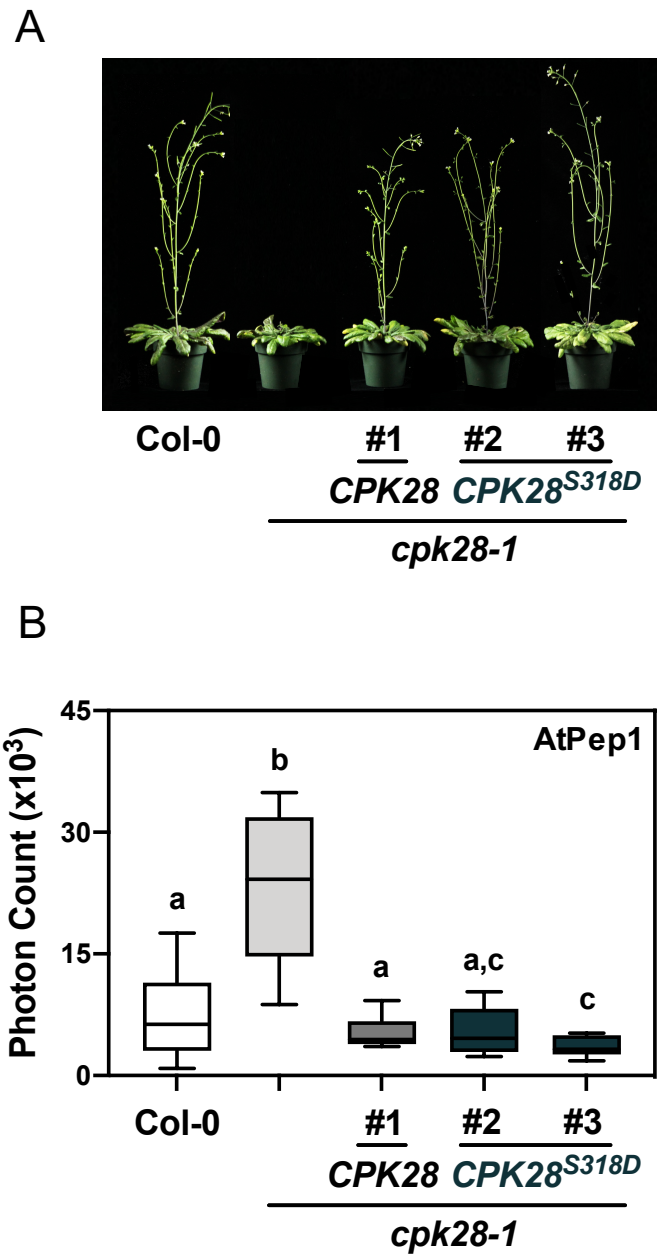

Figure S5. CPK28^{S318D} complements *cpk28-1* in stem elongation and immune-induced oxidative species production. *(A)* Stem elongation of six-week-old Col-0, *cpk28-1*, *cpk28-1/pCPK28:CPK28-FLAG*, and *cpk28-1/pCPK28:CPK28^{S318D}-FLAG* lines. *(B)* Oxidative bursts following treatment with AtPep1 (500 nM). Experiments were conducted exactly as described in Bredow et al., 2019 (1) over 40 min with an integration time of 1000 ms and readings every 2 min. Values represent total photon counts over 40 min and are presented as boxplots indicating first and third quartiles, split by a median line, and whiskers representing maximum and minimum values. Statistically different groups ($p<0.005$) are indicated with lowercase letters, as determined by ANOVA analysis followed by Tukey's posthoc test. Experiments were conducted three times with similar results.

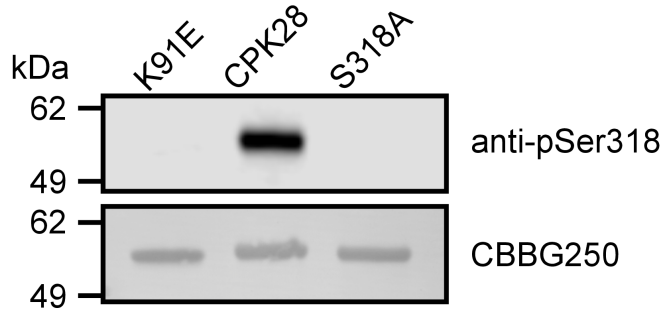

Figure S6. Specificity of the *α*-pSer318 antibody. Specificity of the CPK28 pSer318 antibody was determined by immunoblotting against wildtype (CPK28), kinase-dead ($CPK28^{K91E}$), or $CPK28^{S318A}$. 200 ng of *in situ* phosphorylated purified recombinant protein was separated by gel electrophoresis and blotted to a PVDF membrane before probing with 2 µg/mL anti-CPK28 pSer318 IgGs. Only the wildtype protein was detected, demonstrating specificity of the antibody for the pSer318 site. Gels were stained with Coomassie Brilliant Blue (CBBG250) to assess loading. Experiments were conducted twice with similar results.

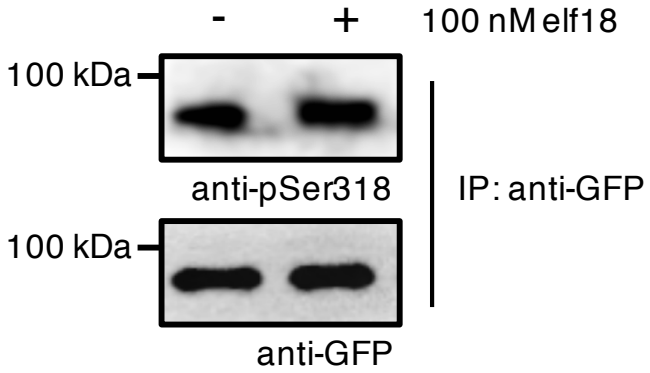

Figure S7. *In vivo* phosphorylation of CPK28-Ser318 is not stimulated by elf18 treatment. 4-week-old *cpk28-1* Arabidopsis plants expressing *35S:CPK28-YFP* were treated with 100 nM elf18 or water for 20 mins prior to protein extraction. CPK28-YFP was immunoprecipitated using anti-GFP beads and detected by immunoblot analysis using anti-pSer318 or anti-GFP antibodies. Experiments were conducted three times with similar results.

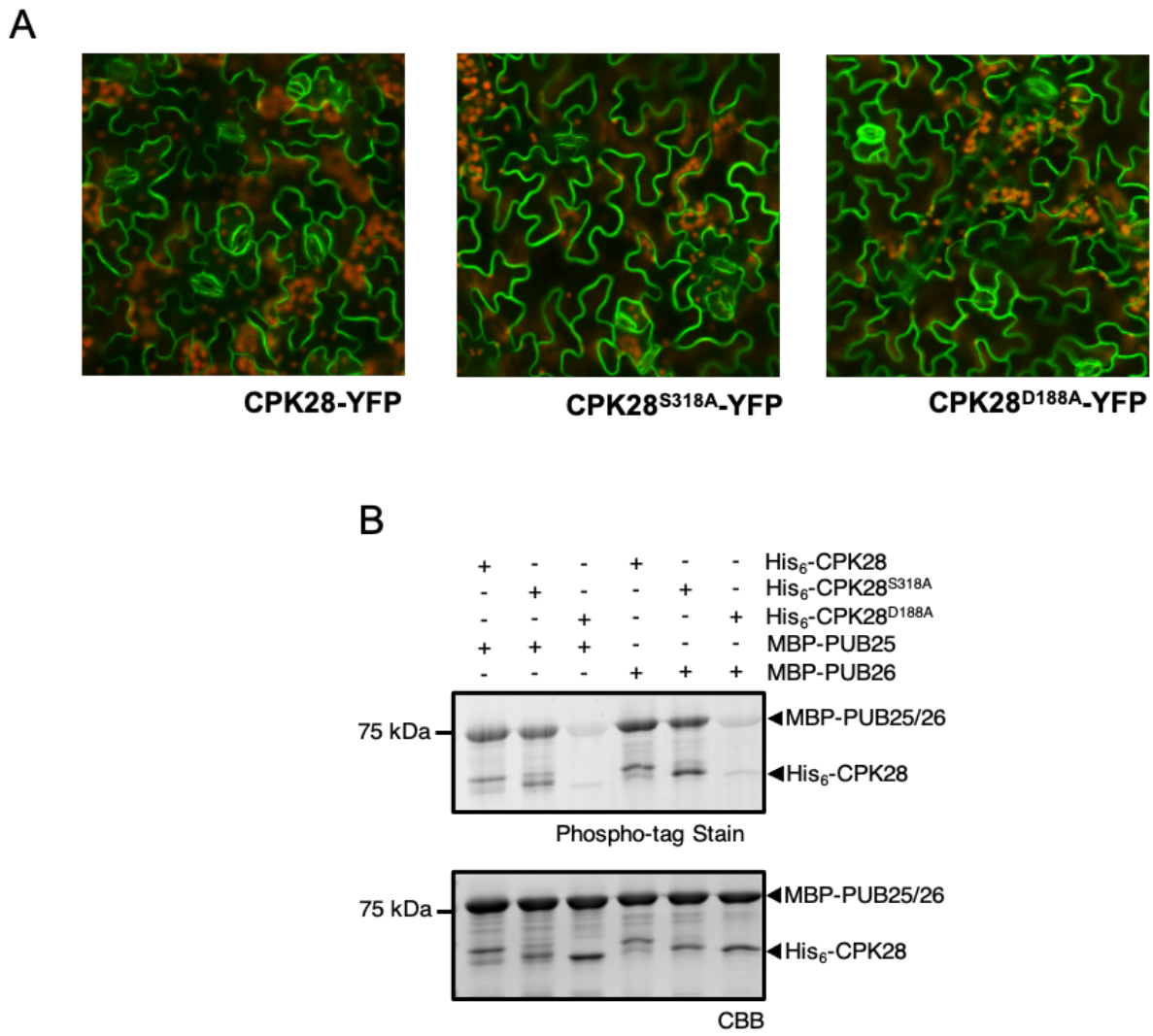

Figure S8. CPK28^{S318A} localizes to the plasma membrane and phosphorylates PUB25 and PUB26. *(A)* Subcellular localization of CPK28-YFP, CPK28^{S318A}-YFP, and CPK28^{D188A}-YFP stably expressed under the CaMV *35S* promoter in *cpk28-1* mutants. Imaging was performed using a LSM 710 (Zeiss) confocal microscope with excitation at 488 nm for yellow fluorescent protein (YFP; coloured green) and a range of 510-540 nm for measuring emission. Chlorophyll autofluorescence (coloured red) was detected with an excitation wavelength of 543 nm and an emission wavelength range of 680-760 nm. *(B)* Phospho-tag gel stain of *in vitro* kinase assay using recombinantly produced His$_6$-CPK28, His$_6$-CPK28^{S318A}, or His$_6$-CPK28^{D188A} and MBP-PUB25 or MBP-PUB26. Gels were stained with Coomassie Brilliant Blue (CBB) to assess loading. Experiments were conducted at least three times with similar results.

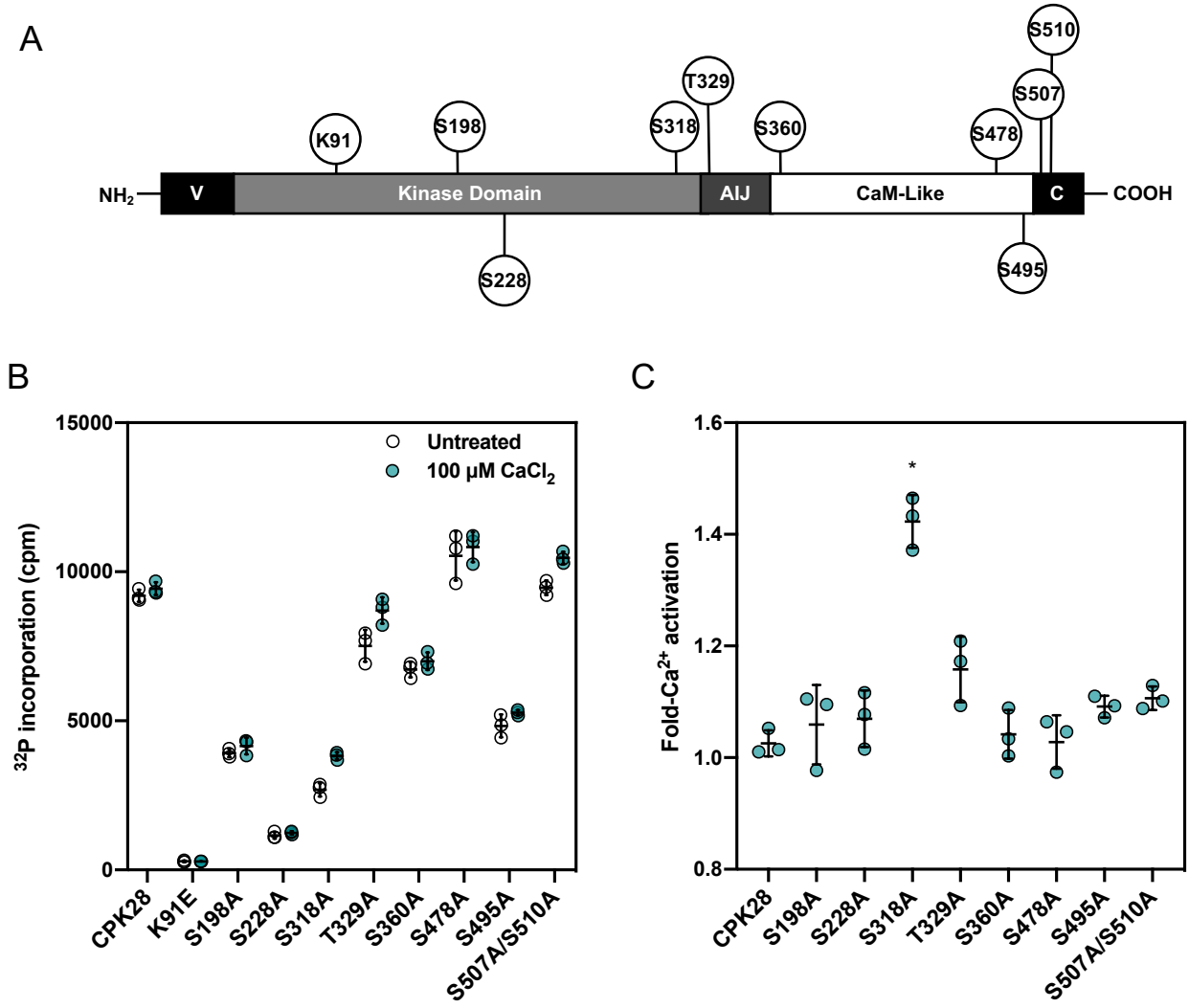

Figure S9. Ser318 phosphorylation uniquely primes CPK28 for Ca^{2+}-activation. *(A)* Position of tested phosphorylation sites across CPK28 protein domains. *(B)* Biochemical screen of CPK28 phospho-ablative null mutants for Ca^{2+} activation of peptide kinase activity using the ACSM+1 peptide as substrate. Activity was assessed using *in situ* phosphorylated purified recombinant proteins at either background (open circles) or 100 µM $CaCl_2$ (teal circles) and is shown as ^{32}P incorporation in cpm. Individual data points (three technical replicates) are shown with mean and standard deviation. *(C)* Fold-activation of CPK28 phospho-ablative null mutants by the addition of excess Ca^{2+} derived from data shown in *(B)*. No difference is observed for wildtype CPK28 between these two conditions and only the S318A site-directed mutants showed statistically significant activation by Ca^{2+} (Kruskal-Wallis ANOVA, p = 0.024361, n = 3 technical replicates). The screen with all phospho-site mutants was performed once and S318A was selected for confirmation of altered calcium sensitivity.

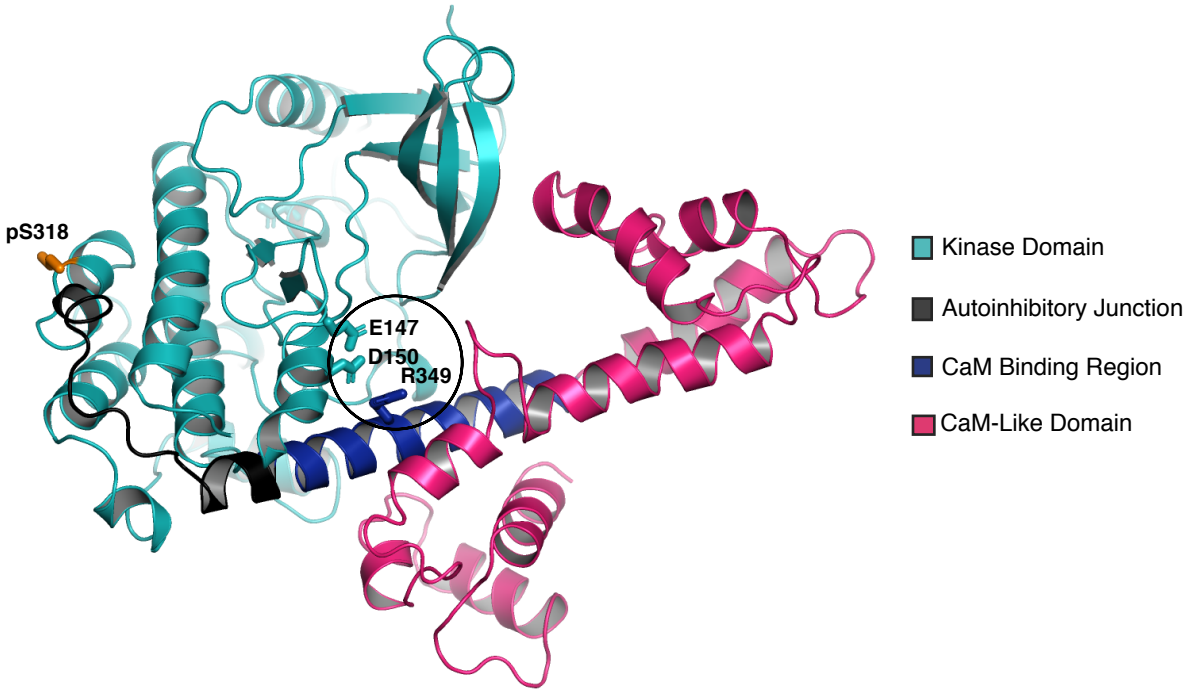

Figure S10. Structural modeling of CPK28. A model for CPK28 was generated using the PHYRE2.0 Protein Recognition Server (2) with inactive TgCDPK1 (iTgCDPK1; 3KU2) as a template (95% confidence score). Phosphorylated Ser318 is indicated in orange. The CaM binding region, located within the autoinhibitory junction (Leu341-Leu362) (3), is indicated in blue. The residues in the autoinhibitory triad that stabilizes TgCDPK1 (Lys338-Glu135-Asp138)(4), corresponding to Arg349-Glu147-Asp150 in CPK28, are labelled. CPK28 was visualized using the PyMOL Molecular Graphics System, Version 2.0 Schrödinger, LLC with PyTMs legacy add-on for post-translational modifications.

Table S1. List of (A) germplasm, (B) constructs, and primers used in this study.

(A)

Genotype	Reference
cpk28-1	Matschi et al., 2013 (5)
bik1	Zhang et al., 2010 (6)
bik1 pbl1	Zhang et al., 2010 (6)
cpk28-1 bik1 pbl1	This study
cpk28-1/pCPK28:CPK28-FLAG line #1	This study
cpk28-1/ pCPK28:CPK28^{S228A}-FLAG line #3	This study
cpk28-1/pCPK28:CPK28^{S228A}-FLAG line #6	This study
cpk28-1/pCPK28:CPK28^{S318A}-FLAG line #1	This study
cpk28-1/pCPK28:CPK28^{S318A}-FLAG line #2	This study
cpk28-1/ pCPK28:CPK28^{S318D}-FLAG line #2	This study
cpk28-1/pCPK28:CPK28^{S318D}-FLAG line #3	This study
cpk28-1/ pCPK28:CPK28^{S495A}-FLAG line #1	This study
cpk28-1/ pCPK28:CPK28^{S495A}-FLAG line #2	This study
cpk28-1/35S:CPK28-YFP	Matschi et al., 2013 (5)
cpk28-1/35S:CPK28^{D188A}-YFP	Matschi et al., 2013 (5)
cpk28-1/35S:CPK28^{S318A}-YFP	Matschi et al., 2013 (5)

(B)

Construct name	Primers used (5'-3') or Reference
pRZ949-pCPK28:CPK28-FLAG	Promoter: FW:5'-atcgGGTACCgggcgacgaggaagaccaactc-3' RV:5'-atcgCCATGGggctctgatgaatcgagaaag-3'
	CDS cloning: FW:5'-actgCCATGGGTGTCTGTTTCTCCGCCATTAG-3' RV:5'-atcgGGATCCCTACTTATCATCATCATCCTTGTAATCTCGAAGATTCCTGTGACC-3'
pET28a(+)-T7:His6-CPK28	Bender et al., 2017 (3)
pET28a(+)-T7:His6-CPK28^{K91E}	Bender et al., 2017 (3)
pRZ949-pCPK28:CPK28^{S228A}-FLAG	FW: 5'-CATTGTTGGTgcgCCTATTATGTG-3' RV: 5'-TCATGGAACCTTTTCCCTG-3'
pET28a(+)-T7:His6-CPK28^{S228A}	FW: 5'-CATTGTTGGTgcgCCTATTATGTG-3' RV: 5'-TCATGGAACCTTTTCCCTG-3'
pRZ949-pCPK28:CPK28^{S318A}-FLAG	FW:5'-GCTGCACAAGCACTAGCACATGCGTGGGTTAGAGAAGGCGGGAATGC-3' RV:5'-GCATTCCCGCCTTCTCTAACCCACGCATGTGCTAGTGCTTGTGCAGC-3'
pRZ949-pCPK28:CPK28^{S318D}-FLAG	FW: 5'-ACAAGCACTAGACCATGCGTGGGTTAGAGAAGG-3' RV: 5'-GCAGCAGTTAGCCGTGC-3'
pET28a(+)-T7:His6-CPK28^{S318A}	FW:5'-GCTGCACAAGCACTAGCACATGCGTGGGTTAGAGAAGGCGGGAATGC-3' RV:5'-GCATTCCCGCCTTCTCTAACCCACGCATGTGCTAGTGCTTGTGCAGC-3'
pRZ949-pCPK28:CPK28^{S495A}-FLAG	FW: 5'-GAGATGGGAAAATAGCCCTGCATGAGTTCA-3' RV: 5'-TGAACTCATGCAGGGCTATTTTCCCATCTC-3'
pET28a(+)-T7:His6-CPK28^{S495A}	FW: 5'-GAGATGGGAAAATAGCCCTGCATGAGTTCA-3' RV: 5'-TGAACTCATGCAGGGCTATTTTCCCATCTC-3'
pET28a(+)-T7:His6-CPK28^{D188A}	FW: 5'-GTCTTGTACATAGAGCTATGAAACCAGAGA-3' RV: 5'-TCTCTGGTTTCATAGCTCTATGTACAAGAC-3'
pRZ949-pCPK28:CPK28^{S318D}-FLAG	FW: 5'-ACAAGCACTAgacCATGCGTGGGTTAGAGAAGG-3' RV: 5'-GCAGCAGTTAGCCGTGC-3'
pET28a(+)-T7:His6-CPK28^{S198A}	FW:5'-GAAACCAGAGAACTTTTTGTTCAAAGCAGCTCAACTAGATTCGCCTCTAAAGG -3' RV:5'-CCTTTAGAGGCGAATCTAGTTGAGCTGCTTTGAACAAAAAGTTCTCTGGTTTC-3'
pET28a(+)-T7:His6-CPK28^{T329A}	FW:5'-GGGTTAGAGAAGGCGGGAATGCTGCTGATATCCCTGTCGACATTTCAGTTC-3' RV:5'-GAACTGAAATGTCGACAGGGATATCAGCAGCATTCCCGCCTTCTCTAACCC-3'
pET28a(+)-T7:His6-CPK28^{S360A}	FW:5'-CAATTTGCTTTAAGGGCGCTTGCTGCCACACTTGACGAGGCAGAGATCTC-3' RV:5'-GAGATCTCTGCCTCGTCAAGTGTGGCAGCAAGCGCCCTTAAAGCAAATTG-3'
pET28a(+)-T7:His6-CPK28^{S478A}	FW:5'-GAATGCACACGGGGTTAAGAGGAGCAATAGATCCACTGCTGGATGAAGC-3' RV:5'-GCTTCATCCAGCAGTGGATCTATTGCTCCTCTTAACCCCGTGTGCATTC-3'

pET28a(+)-T7:His6-CPK28$^{S507A/S510A}$	FW:5'-GTTCAGGAGACTTCTAAGAACAGCGGCCATAAGTGCACAGAGAGCACCAAGCCC-3' RV:5'-GGGCTTGGTGCTCTCTGTGCACTTATGGCCGCTGTTCTTAGAAGTCTCCTGAAC-3'
pMAL-c2x:MBP-PUB25	FW:5'-AATCTCTAGAATGCCTAGGAATATAGAACC-3' RV:5'-GATTCTGCAGTCAAAAAGGGACCACTTGG-3'
pMAL-c2x:MBP-PUB26	FW:5'-AATCTCTAGAATGCCGGGGAATTTAGAGCC-3' RV:5'-GATTCTGCAGTCAAAACGGCGCCACTTCGC-3'
pGex6.1-T7:GST-BIK1	FW:5'-TCGAGCGGCCGCATCGTGACATGGGTTCTTGCTTCAGTTC-3' RV:5'-GCGAGGCAGATCGTCAGTCACACAAGGTGCCTGCCAAAAG-3'
pGex6.1-T7:GST-BIK1$^{K105A/K106A}$	FW:5'-TCGAGCGGCCGCATCGTGACATGGGTTCTTGCTTCAGTTC-3' RV:5'-GCGAGGCAGATCGTCAGTCACACAAGGTGCCTGCCAAAAG-3'
pXCSG-35S:CPK28-YFP	Matschi et al., 2013 (5)
pXCSG-35S:CPK28^{D188A}-YFP	Matschi et al., 2013 (5)
pXCSG-35S:CPK28^{S318A}-YFP	Matschi et al., 2013 (5)

Dataset S1. Amino acid sequences of group IV CDPKs across the plant lineage.
This text file includes all FASTA-formatted sequences retrieved following a query for group IV CDPKs using the Phytozome v12 BLAST tool (114 sequences from 53 species).

Dataset S2. Amino acid sequences of representative group I, II, and III CDPKs across the plant lineage.

This text file includes 327 FASTA-formatted sequences retrieved from the Phytozome 12 BLAST tool following a query for group I, II, and III CDPKs in 12 species spanning the plant lineage (*M. polymorpha, P. patens, S. fallax, S. moellendorffi, A. trichopoda, O. sativa, A. thaliana, V. vinifera, R. comunis, B. rapa, T. cacao,* and *M. truncatula*).

SI References

1. M. Bredow, I. Sementchoukova, K. Siegel, J. Monaghan, Pattern-Triggered Oxidative Burst and Seedling Growth Inhibition Assays in Arabidopsis thaliana. *J. Vis. Exp.* (2019) https:/doi.org/10.3791/59437.

2. L. A. Kelley, S. Mezulis, C. M. Yates, M. N. Wass, M. J. E. Sternberg, The Phyre2 web portal for protein modeling, prediction and analysis. *Nat. Protoc.* **10**, 845–858 (2015).

3. K. W. Bender, *et al.*, Autophosphorylation-based Calcium (Ca) Sensitivity Priming and Ca/Calmodulin Inhibition of Ca-dependent Protein Kinase 28 (CPK28). *J. Biol. Chem.* **292**, 3988–4002 (2017).

4. A. K. Wernimont, *et al.*, Structures of apicomplexan calcium-dependent protein kinases reveal mechanism of activation by calcium. *Nat. Struct. Mol. Biol.* **17**, 596 (2010).

5. S. Matschi, *et al.*, Function of calcium-dependent protein kinase CPK28 of Arabidopsis thaliana in plant stem elongation and vascular development. *Plant J.* **73**, 883–896 (2013).

6. J. Zhang, *et al.*, Receptor-like cytoplasmic kinases integrate signaling from multiple plant immune receptors and are targeted by a Pseudomonas syringae effector. *Cell Host Microbe* **7**, 290–301 (2010).